AIMS Geosciences

AIMS Geosciences, 4 (1): 36–65.
DOI: 10.3934/geosci.2018.1.36
Received: 18 December 2017
Accepted: 19 March 2018
Published: 23 March 2018

http://www.aimspress.com/journal/geosciences

Research article

Geoinformatic analysis of vegetation and climate change on intertidal sedimentary landforms in southeastern Australian estuaries from 1975–2015

Ali K. M. Al-Nasrawi[1,*], Sarah M. Hamylton[1], Brian G. Jones[1] and Ameen A. Kadhim[2]

[1] GeoQuEST Research Centre, School of Earth and Environmental Sciences, University of Wollongong, NSW 2522, Australia
[2] Department of Geography, Environment and Spatial Sciences, Michigan State University, Michigan, USA

* **Correspondence:** Email: briangj@uow.edu.au.

Abstract: Vegetation canopies represent the main ecosystems on intertidal landforms and they clearly respond to changes in coastal environments. Climate change, including temperature, precipitation and sea level rise, are affecting the health and distribution of coastal vegetation, as well as the runoff and sedimentation rates that can impact coastal areas. This study has used the normalized difference vegetation index (NDVI) to investigate vegetation canopy dynamics on three different coastal sites in southeastern Australia over the past 47 years (1975–2015). NDVIs temporal-datasets have been built from satellite images derived from Landsat 1–8. These were then regressed to the climatic and geomorphic variables. Results show clear increases in NDVI at Towamba and Wandandian Estuaries, but a decline at Comerong Island (southeastern Australia). The sedimentation rate has the most significant positive impact on NDVI since it has the potential to provide additional space for vegetation. Temperature and sea level rise have positive effects, except on Comerong Island, but rainfall has no significant effect on the NDVI at any site. Different NDVI trends have been recorded at these three coastal sites reflecting different correlations between the vegetation, climatic and geomorphic (as independent) variables. The geomorphological characteristics of the highly-dynamic intertidal estuarine landforms, which are subject to active erosion and deposition processes, have the largest impact on vegetation cover and, hence, on NDVI. Assessing the vegetation canopy using NDVI as an evaluation tool has provided temporal-dynamic datasets that can be correlated to the main individual environmental controls. Such knowledge will allow resource managers to make more informed decisions for sustainable conservation plans following the evaluation the potential consequences of any environmental changes.

Keywords: ecosystems; climate change; vegetation response; NDVI; GIS analyses; remote sensing; satellite imagery

1. Introduction

There is much concern about climate change impacts on the Earth's ecosystems [1–4]. The clearest and widest ecosystem responses to climate change are represented in the vegetation canopy dynamics of such ecosystems [5,6]. At global, regional and local landscape scales, vegetation responses are affected by whichever climatic factors represent the dominant limitation to plant growth [6]. In a coastal-dynamic context, changes in vegetation conditions can be categorised as those affected by temperature and precipitation that impact growth and productivity, as well as those that affect the landform stabilities, including sea level and sedimentation dynamics [7–11].

Coastal ecosystems and, specifically, wetland habitats are highly productive natural ecosystems [12,13]. Coastal wetlands are also the most sensitive and responsive coastal ecosystems to environmental pressures, such as climate change, the rising sea level and the current stage of human settlements, which control most of the coastal processes [8,14–16]. Coastal ecosystems may be affected by a local surge in surface temperature, precipitation decline, and sea level rise (SLR) under current climate scenarios. In addition, human activities have been shown to have a substantial effect on coastal ecosystems (e.g., via habitat destruction and biodiversity reduction) [17], which implies that there is a great need to detect and predict changes in ecosystem functioning.

Coastal environmental studies have become more focused on the applications of climate change scenarios within the coastal zones to assess the vulnerability of its ecosystems and/or landforms [1,5,10,15,18,19]. So far, these studies have indicated an important climate—eco-geomorphic correlation. However, limited discussion has focused on examining the vegetation trends associated with climate-related factors at specific geomorphic-estuarine sites in coastal wetlands. This case study from the southeastern Australian coast shows the relationships between vegetation and different environmental conditions, geomorphic and human pressures; it demonstrates the applicability of these methods to other ecosystems worldwide.

The aims of this exploratory study are to:

i) Quantify temporal changes in the extent of coastal vegetation canopies, and
ii) Evaluate the spatial distribution of changes within sensitive wetland landforms.

These aims were achieved by analysing the vegetation trends over time and establishing correlations between change stressors and the vegetation response, which can be used to predict future response scenarios for such landscapes along the southeast Australian coast. The research objectives have been based on a literature review augmented by imagery modelling (using RS and GIS) and subsequent statistical analysis to provide a quantitative outcome that can be used to offer possible sustainable management solutions with potential worldwide applications.

To have a comprehensive practical view of the above correlations, this paper has focused on three southeast Australian estuaries, as ideal case studies. Australian southeastern coastal ecosystems in the temperate zone have experienced considerable vegetation dynamicity during the last few decades of climate change, particularly after the 1980s. An investigation of the relationships between vegetation dynamics and climate change is urgently required for coastal zone management, and these empirical case studies illustrate concepts that could be useful and applicable worldwide. Available satellite

imagery allows us to perform these analyses for the past four and a half decades using GIS. Linear regression and correlation analysis can then be used to assess the correlations between each of these three vegetation dynamic study sites and the climatic indicators: Temperature, precipitation and sea level rise, as well as with human impacts. Anthropogenic impacts have directly affected the amount of sediment reaching the estuary from the catchments, as well as any direct anthropogenic modifications caused by habitation within the coastal environment. More specifically, modelling the relationship between NDVI and the environmental conditions across 40 years, for each site on the southeastern Australian coast, has been based on: (i) NDVI trend analysis; (ii) a correlation regression model; (iii) NDVI change map distributions. This study has used the NDVI index to assess spatial and temporal changes of vegetation radiation at chosen coastal sites. These vegetation multispectral wave reflections were then regressed with the related climatic and geomorphic trend factors (temperature, rainfall, sea level rise and sedimentation rates).

1.1. Study sites' general setting

This research has selected three sensitive coastal ecosystems on the southeastern Australian coast (Figure 1) that are vulnerable to climate change outcomes and they can be considered representative of worldwide ecological responses [20–23].

The southeast Australian coastline includes protected lagoons, open bays and wave-dominated beach natural assets that make a vast contribution to the economy [24–26]. Estuarine ecosystems at Towamba, Wandandian delta, and Comerong Island provide representative case studies of ecosystem responses under different wave-energy regimes ([16,17,27,28]; Figure 1).

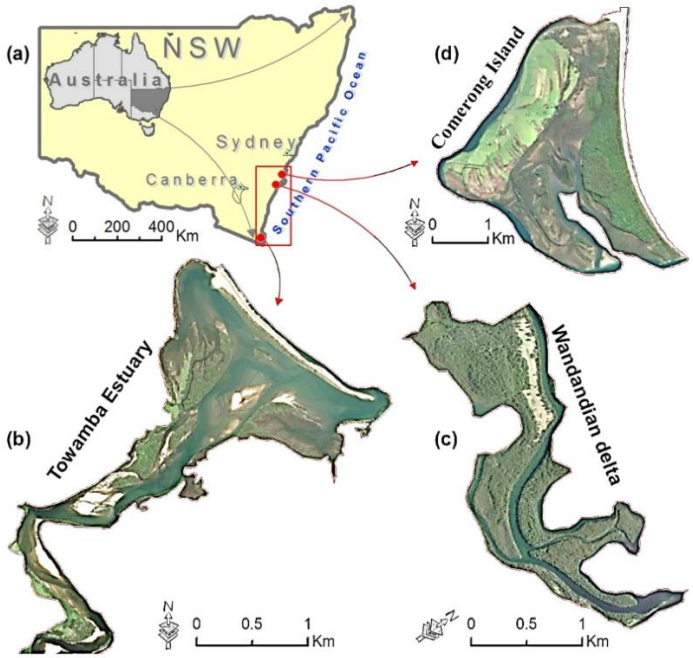

Figure 1. (a) Study site locations along the NSW coast in southeastern Australia. From south to north they include the (b) Towamba estuarine ecosystem in Twofold Bay; (c) Wandandian estuarine delta in St Georges Basin; (d) estuarine portions of Comerong Island on the open wave-dominated coast.

1.1.1. Towamba estuary

Located 486 km south of Sydney on the far south coast of New South Wales (NSW; 37°06'38.0"S 149°54'10.7"E, Figures 1a and 1b) with a temperate oceanic climate (Cfb), the Towamba catchment has no distinct dry season, with average temperatures ranging from 11 ℃ in winter (July and August) to 20 ℃ during summer (January and February), and an average precipitation of 882 mm annually [29]. The Towamba River has built its specific estuarine eco-geomorphic system at the meeting point between the high-elevation and steep mountains/catchment area and a large open bay on the Pacific Ocean [27,30–32]. Although this estuary ecosystem is only 2 km^2 it receives a very large amount of sediment annually from the steep terrain and mostly untouched catchment of 1034 km^2 [26,31]. The estuary is mostly surrounded by rocky outcrops that have limited estuary growth. This has resulted in forcing the sediment accumulation and growth to occur in the middle and open-water sides of the estuary, leading to a narrow main active channel and forcing the barrier island to grow seawards [27,30–32]. According to Roy *et al.'s* [26] classification, it is a wave-dominated barrier estuary in the mature stage of ecosystem development. It has an open estuary mouth into Twofold Bay in the Tasman Sea discharging water and sediment mainly derived from the Nullica State Forest (national park) and other untouched forests in the catchment area. The source of the perennial Towamba River is at Mount Marshall in the South Coast Range, which forms part of Great Dividing Range [26,31]. The river flows generally southeast and then northeast, joined by twelve tributaries, including Mataganah Creek and Wog-Wog River, before reaching its mouth and emptying into Twofold Bay just southeast of Eden near East Boyd. The river descends 533 m over its 86 km course [26,31].

1.1.2. The Wandandian estuarine delta

Located about 200 km south of Sydney, in the western corner of St Georges Basin (35°06'23.9"S 150°33'21.8"E, Figures 1a and 1c), it has a temperate oceanic climate (Cfb) with no dry season and average temperatures ranging from 11.5 ℃ in winter (July and August) to 21 ℃ during summer (January and February, data from "Sussex Inlet Bowling Club" gauging station; [29]), average precipitation is 1264 mm annually, with 400 mm estimated runoff [28,29,33]. The delta area is about 3.1 km^2 while its catchment is approximately 152 km^2 [28,31]. The Wandandian delta developed during the Holocene and consists of fluvial sediments (gravel, sand, silt and clay) and it is still growing [33]. Wandandian Creek is the main water and sediment supplier to the delta, being 125 km long, extending from the Tianjara Range (part of the Australian Great Dividing Range) before discharging into St Georges Basin [28,33].

1.1.3. Comerong Island

Located about 30 km north of the Wandandian site on the mid-NSW coast (34°53'08.2"S 150°44'14.3"E, Figures 1a and 1d), Comerong Island has a warm oceanic to humid subtropical climate (Cfa), with no dry season and a hot-warm summer [29]. The average temperature ranges from 16 ℃ in winter (July and August) to 25 ℃ during summer (January and February, data from "Greenwell Point Bowling Club" gauging station; [29]) and the average precipitation is 1127 mm annually, with 350 mm estimated runoff [29]. Comerong Island is about 4.5 km^2 in area, and is located at the end of the Shoalhaven River near Crookhaven Heads forming a barrier-deltaic island on the

NSW open coast [17]. Comerong Island has been internationally recognized as a habitat for a range of waders and shorebirds, and it has an amazing wetland distribution consisting of mangroves and saltmarshes [16,17,34]. At the same time, it represents a clear example of an ecosystem affected by human influences (associated with a developed catchment) accompanied by sea-level rise resulting in changing shorelines and vegetation extent [21,34,35]. Geomorphically, the island developed as a small estuarine barrier at the mouth of the Shoalhaven River during the mid-Holocene by fluvial sedimentation behind the marine sand barrier [36]. The delta migrated northwards and the entrance was frequently blocked so, in 1822, Alexander Berry constructed a canal that linked the Shoalhaven and Crookhaven Rivers (~4 km south of the old river entrance) to alleviate the high river water levels that threatened the estuary and all associated human settlements [37]. This resulted in the final shape of Comerong Island, but the lower water levels threatened some island ecosystems, such as saltmarsh areas [17].

1.2. Climatic conditions along the southeast Australian coast

The Australian east coast is subject to varying climate conditions over a substantial land scale, variable geology, air/sea currents, and different coastal environmental systems, making deductions difficult in light of the Köppen climatic framework [18,38,39]. Thus, the Australian Bureau of Meteorology has modified the Köppen classification system to meet the local specifications [29].

The eastern coast of Australia has north-south stretched climate zones, affected by the coastal wave-dominated air/ocean currents, especially the warm East Australian Current. Thus, the tropical and subtropical weather conditions are stretched farther south than normal. This could also be enhanced by global warming, which causes similar shifts in many parts of the world. This has caused a range of unstable weather events, such as cyclones, floods, droughts, and other sporadic natural disasters at the study sites or in their catchments, which have caused damage costing millions of dollars annually [18,29,40,41].

Interestingly, while the eastern Australian coast is prone to such climate changes, their recurrence intervals are liable to become more frequent and intense. Present and future vegetative changes, the present rate of ocean level rise, and the accompanied immersion of eastern Australian low-lying waterfront habitats (e.g., estuaries and coastal wetlands) are affected differently at present, and are anticipated to change as a result of global warming [6,29,41].

1.2.1. Precipitation variation along the eastern Australian coast

Precipitation records have a tendency to fluctuate along the east Australian coast, especially on the southern NSW coast, where all three study sites are located [29,40]. However, the Australian general climate indicators, including those on the southeastern coast, show a clear trend of declining precipitation over the last few decades, which is part of the global climate trend (Figure 2; [39]). The Towamba estuarine ecosystem receives an average precipitation of 882 mm annually (Figure 2a; [29], data from the "Marine Rescue Eden" gauging station, located 1.4 km away from the estuary). The overall average Towamba precipitation trend shows a slight decline during the last forty years (Figure 2a), from 974 to 879 mm (2.38 mm/a). In contrast, the Wandandian deltaic ecosystem receives annual average precipitations of 1264 mm (Figure 2b; [29]; data from "Sussex Inlet Bowling Club" gauging station, located 11.2 km away from the delta). The overall average Wandandian precipitation

trend shows a significant declined over the last forty years (Figure 2b), from 1350 to 952 mm (9.95 mm/a). The Comerong Island estuary receives an average precipitation of 1127 mm annually (Figure 2c; [63]; data from "Greenwell Point Bowling Club" gauging station, located 0.4 km away from the island) and the overall average Comerong precipitation trend has also declined during the last forty years (Figure 2c), from 1203 to 1026 mm (4.43 mm/a).

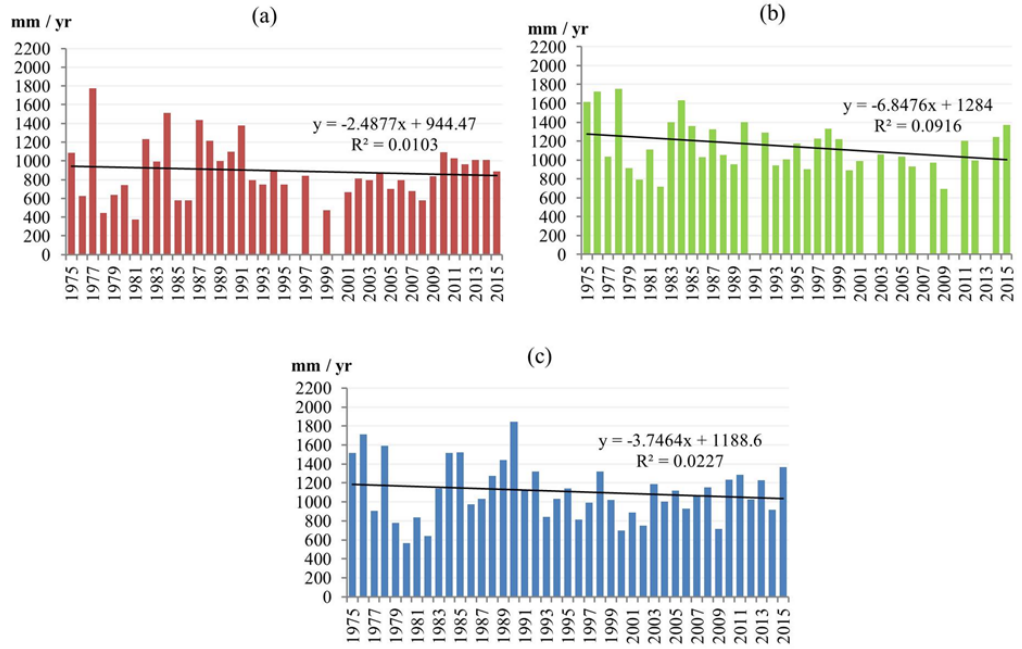

Figure 2. Annual precipitation records (1975–2015) at the study sites: (a) Annual precipitation trends of Towamba estuary; (b) Annual precipitation trends of Wandandian delta; (c) Annual precipitation trends of Comerong Island. The overall trends show a decline in precipitation over the study sites during the past forty years [39,42]. *Note, the overall trend is presented by the grey line on (a)–(c).

There is also a clear decrease in precipitation along the coast from north to south that could be related to the regional and global precipitation distributions, which usually decrease towards higher latitudes. However, the case study sites, which are located at different latitudes and receive different amounts of precipitation, all show a similar decline in the overall records from 1975 to 2015 (Figure 2).

1.2.2. Temperature

Increasing the overall temperature will affect plant productivity and the growing season length, and these affects should be clearly indicated in the measured NDVI records. The mean annual temperature data for the last five decades (1966–2016) at the case study sites have been analysed (Figure 3). At these sites air temperature has clearly increased (Figure 3), representing the combined effects of local and regional global warming trends, and would have a positive impact on vegetation growth especially in coastal ecosystems with enough water resources, like wetlands [6,41,43]. Figure 3 shows that the average air surface temperature has fluctuated, but shows a rising trend within the last

few decades over all three case studies. The Towamba estuarine ecosystem (with Cfb weather conditions) is the highest latitude site that records higher global warming impacts and, as Figure 3a shows, while the mean temperature is 16 ℃ the overall trend has increased by 0.4 ℃, from 15.8 ℃ to 16.2 ℃. The Wandandian estuarine delta (with Cfb weather conditions) has a temperature average of 16.5 ℃ with a slight increase of 0.2 ℃, from 16.4 ℃ to 16.6 ℃ (Figure 3b), while the Comerong Island estuary (with Cfa weather conditions) has a slightly increased temperature trend by 0.2 ℃ as well, ranging between 16.5 ℃ and 16.7 ℃, with an of average of 16.6 ℃ (Figure 3c).

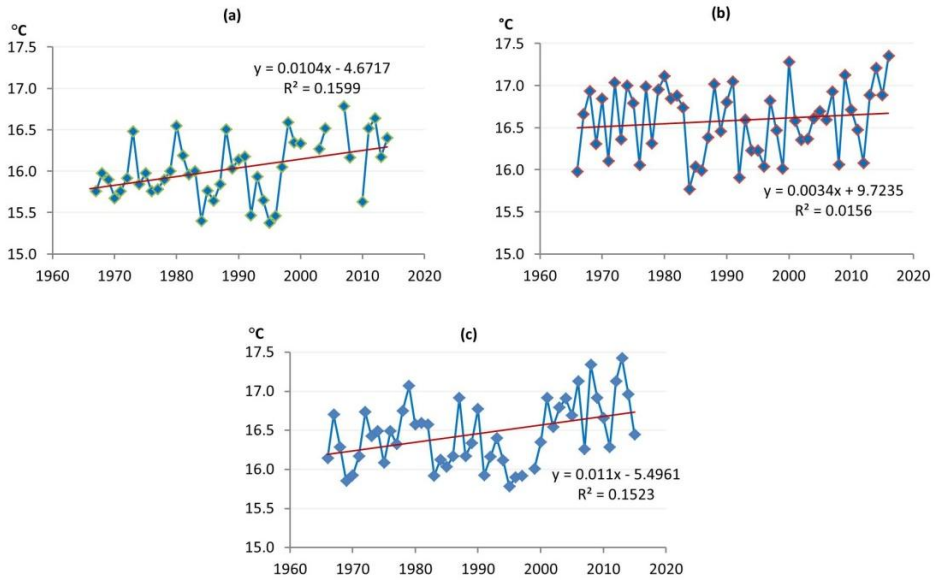

Figure 3. Mean annual air Celsius temperature (1968–2015) at the study sites: (a) Annual temperature average and trends of Towamba Estuary; (b) Annual temperature average and trends of Wandandian delta; (c) Annual temperature average and trends of Comerong Island. The temperature trends at the three study sites have increased during the past 49 recorded years [39,42].

The results of monthly (mean) temperature and precipitation data for all three study sites have been analysed and are shown in Figure 4. They indicate that January and February (southern hemisphere summer) are the warmest months, while February and March are the wettest months in the records (Figure 4). The monthly precipitation records show that these sites have no dry season, but precipitation declines slightly during winter, especially from July to September (Figure 4).

The ecosystem related measures that can be acquired from an NDVI dataset can be confused or reliable according to the ecosystem issues under consideration. Within areas where a variable rainy season is present, the analysis should concentrate on the more stable and less vegetation dynamic season (summer) to determine the NDVI from the remote sensed data [44,45]. Using NDVIs from the peak vegetation-growing months of January and February, combined with the more stable hydrodynamic conditions at this time of year, will minimise the variability of the vegetation reflections and the catchment influences in such intertidal coastal ecosystems. These two months have the highest NDVI values recorded during the long warm growing season. This summer period is associated with enough water resources: (i) brackish water in the intertidal habitats (e.g., mangrove and saltmarsh); (ii) precipitation for the elevated vegetation on the estuarine barrier (Towamba and Comerong, ca. 4–6 m

above sea level) and the high deltaic zone (Wandandian, ca. 3–4 m above sea level) where some mixed native plants, like eucalyptus, are present and are rainfall-dependent [17,28,43–45].

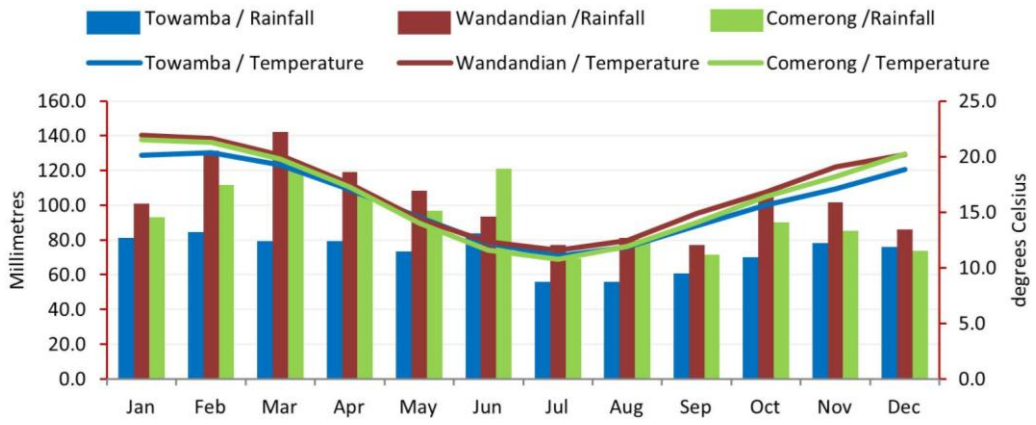

Figure 4. The monthly data of temperature and precipitation for all study sites (together) during 1966–2015 show that the highest seasonal temperature occurs during the southern hemisphere summer, particularly in January and February. At the same time, February and March are the wettest months in the records [39,42].

1.2.3. Mean sea level

Coastal ecosystems, particularly coastal wetlands (e.g., mangrove, salt marsh and associated habitats) will be strongly influenced by sea level rise (SLR) in terms of their zonation, position and elevation characteristics [7,46,47]. These habitats can be subjected to losses of areal extent, and distribution, as well as the wellbeing of productivity [48,49]. They are the most sensitive, responsive, and vulnerable ecosystems on Earth to SLR [11,17]. Coastal wetland ecosystems are well developed and conserved along the extensive Australian coasts and shorelines, including southeastern NSW [14,26,50]. However, changes are not exclusively restricted to SLR since, nowadays, direct and indirect climate change and human development have had significant impacts on such ecosystems worldwide [8,47,49].

Stratigraphic and sedimentological studies of the sediments underlying coastal wetlands and their unique associated habitats (e.g., mangrove and salt marsh) indicate that there have been considerable changes in the extent of these wetlands as a direct result of historical sea level fluctuations [7,8,51,52]. In addition, the indirect human settlement effects of modifying the catchments have led to a series of sedimentary problems, which would leave the coastal wetlands less able to keep up with SLR [17,49].

In general, as observed from prior studies, stressors would, in either a direct or indirect way (or both), lead to losses of coastal wetland vegetation extent, surface canopies and land classes. Hence, the response of coastal ecosystems, especially coastal wetland ecosystems, to SLR would depend on the existing coastal topography, together with rates and sources of sedimentation, and the SLR rate itself [1,8,19,53].

The local reported mean sea level rise (MSLR) that is relevant to the study sites forms part of the global sea level rise resulting from global climate change [46,54]. It is based on the mean sea level relative to the local or nearest tide gauging stations to the case study sites as follows: The Towamba site has used the Eden tidal gauge station (1.4 km away) and the available observation

period is from 1986 to the present time. Sea level data for both the Wandandian and Comerong sites was derived from the Port Kembla tidal gauge, located ~45 km away, but it has a longer observation record extending from 1957 to recent times [55], but has some unavailable observations in 1957–1958, 1960–1972, 1983–1984 (Figure 5).

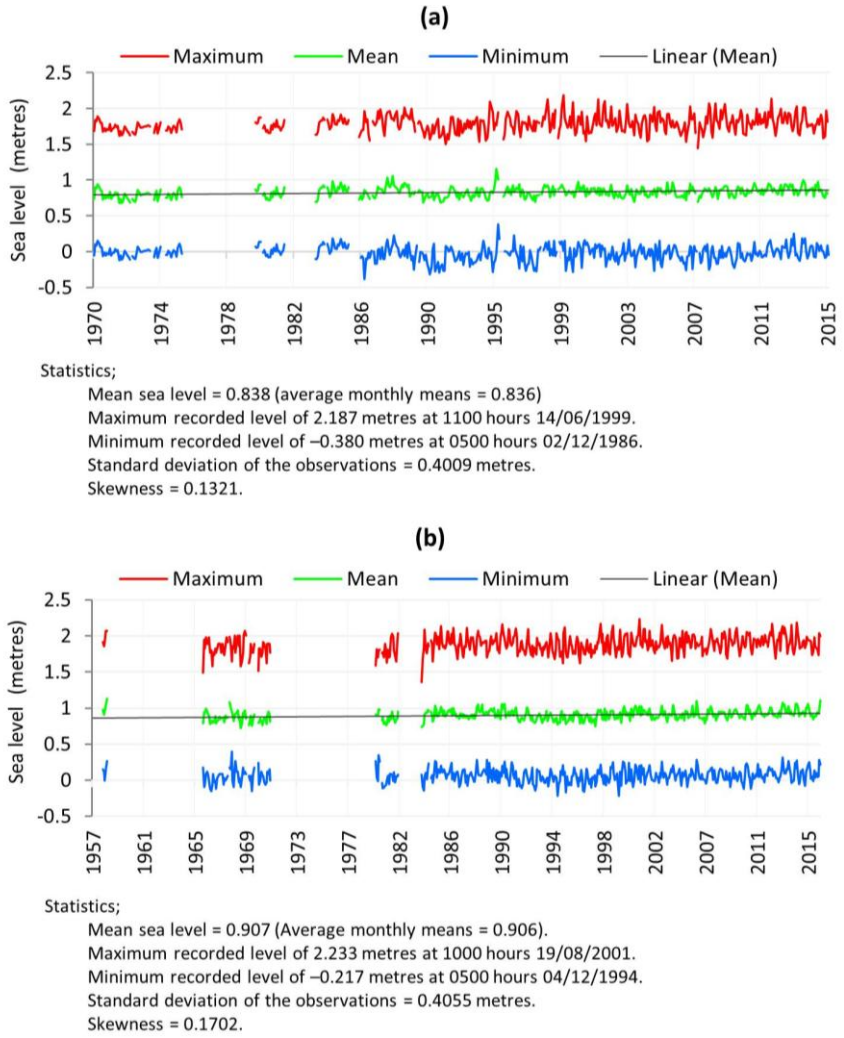

Figure 5. (a) Monthly sea level records (the tidal range in m) for the Towamba estuarine ecosystem (Eden; 1986–2015); (b) Wandandian estuarine delta and Comerong Island estuary (Port Kembla; 1957–2016). Red is the maximum, green is the mean, and blue is the minimum [55].

Primary analysis of these monthly data from the above gauging stations, based on the 59-year time-series of sea-level measurements from 1957 to 2016 at Port Kembla, conceded a statistically notable SLR trend during the past few decades. The standard deviation of data observations is equal to 0.4 at both gauging stations [29]. Figure 5 clearly shows that sea level at both gauging stations has fluctuated and risen as follows: At the Towamba site; the average mean sea level fluctuation is 0.84 m annually, whereas, the overall average trend of SLR at Towamba is a rise of 4.5 cm during the last three decades, from 0.815 to 0.860 m.

For the Wandandian and Comerong sites the annual average mean sea level is 0.907 m, whereas,

the overall average trend of SLR at Wandandian and Comerong is 3.5 cm during the past six decades, from 0.895 to 0.930 m. The NDVI datasets have been analysed at five year intervals from 1975–2015. Thus, the average SLR data over each five year interval is used in the regression model to assess their correlation with the NDVIs.

2. Methodology and dataset collection

The main methods used in this study are GIS modelling and statistical analyses, which have been applied to the three case studies for the period from 1975–2015 at five-year intervals, as follows (see Figure 6):

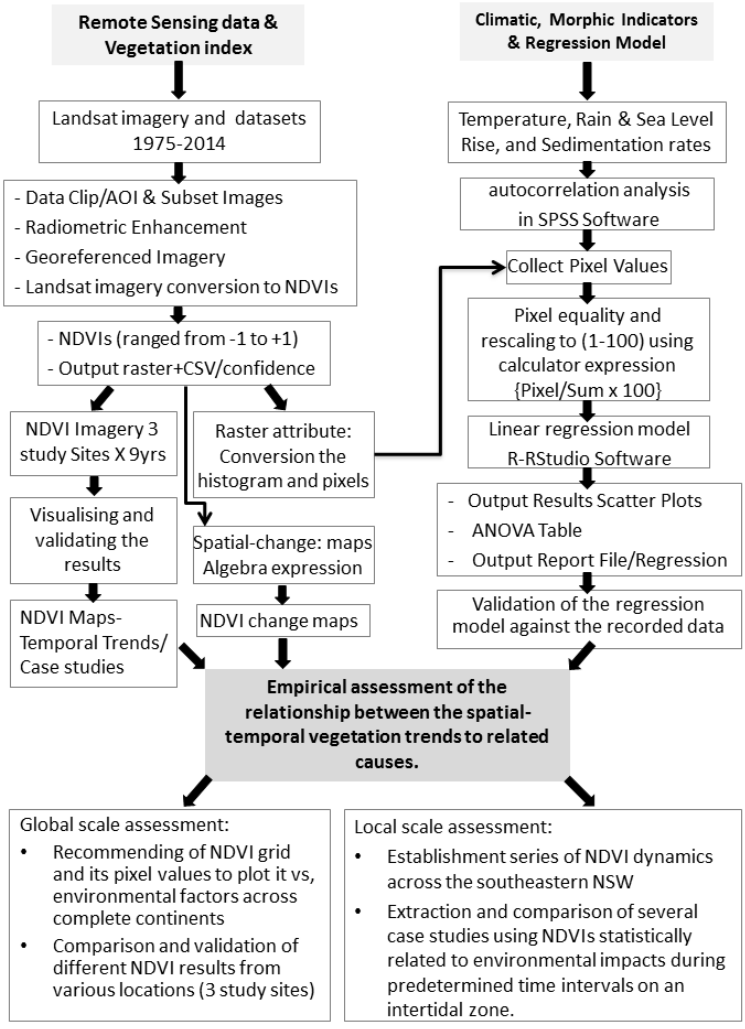

Figure 6. Methodology of the modelling approach steps used in the study. It has been applied to the Landsat satellite imagery and climatology datasets, using ERDAS IMAGINE 2014, ArcGIS 10.2 and R-RStudio.

- The GIS analysis was based on imagery analyses for NDVI, including imagery spatial/radiometric enhancements, classification indices, clipping/expression, temporal trend analysis, and raster attribute analysis (collecting the pixel values for the statistical analysis).

- The statistical analysis using RStudio included analysing the climatic indicator trends for precipitation, temperature, and mean sea level, as well as regression analysis to determine the liner correlation between these climatic factor trends and the NDVI trends (pixel values) spatio-temporally.

2.1. Landsat imagery data (1975–2015)

Landsat 1–8 imagery at five-year intervals from 1975 to 2015 (Table 3) was utilised to create the NDVIs to determine vegetation trends for each case study site. The analysis was based on a Landsat MSS, TM sensor summer dataset with a resolution of 79 m or 30 m from a single satellite image covering each site/each year. The imagery was chosen from southern hemisphere summer images since they have the best weather conditions that may affect the surface/canopy radiation wave reflections recorded by the satellite, particularly within such coastal ecosystems at the case study sites.

Table 3. Landsat satellite sensors utilized for the case studies*.

Sensor	Satellite	Overpass/orbit Frequency	Data Record (years)	Spatial Resolution
MSS/RBV	Landsat 1–3	18 days	Jan, Feb 1975, and 1980	79 m
NSS/TM	Landsat 4–5	16 days	Jan, Feb 1985, 1990, and 1995	30 m
ETM+, OLI	Landsat 7–8	16 days	Jan, Feb 2000, 2005, 2010, and 2015	30 m

*: [56,57].

The Landsat images have been radiometrically and geometrically rectified to meet the framework parameters, including coordinate systems, atmospheric issues, and pixel size, as well as clipping the Landsat datasets (1975 to 2015) for all three case study sites, according to each site boundary to be presented separately, but the whole data for the pre-chosen year and from the 4 preceding years will be included in the processes to obtain the average NDVIs for that chosen year [45,58–60].

As part of the correction stage of Landsat images, the digital numbers (DN) were corrected to radiance values through the following steps:

1- Radiance = gainDN + offset

2- Radiance = (LMAX − LMIN)/255DN + LMIN, however, these corrections could change with time and can be obtained from the CPF archive. Then, radiance is converted to TOA reflectance using Eq (1):

$$\boldsymbol{\rho_p} = \frac{\boldsymbol{\pi} \cdot \boldsymbol{L_\lambda} \cdot \boldsymbol{d^2}}{\boldsymbol{ESUN_\lambda} \cdot \boldsymbol{\cos\theta_s}} \quad (1)$$

Where; *p* is the unitless planetary reflectance, *L* is the spectral radiance in astronomical units, *Esun* is the mean solar exo-atmospheric irradiance, and *s* is the solar zenith angle in degrees. Meanwhile, to make the multi-date data comparable for valid use in research, this paper has used the assuring geometric accuracy, including scaling of pixel sizes to a uniform spacing and converting the imagery pixels (30 and 79 m) to be equally scaled from 0 to 100 (especially needed when using MSS, TM, and OLI, with different native bit depths) assuring common pixel extents. Part of the standard procedure, statistical weighting, is used to cope with rescaling to a common pixel spacing to accommodate images across multiple dates. Using the standard procedure for coming to a uniform

spatial scale would require some kind of neighbourhood weighting, where the respacing comes before the analysis, which is usually used to make sure that the output values are radiometrically equivalent, rather than visually smooth. That determines the weighting used. The results of analysing the various resolutions of the Landsat datasets (Table 3) guided this study to develop a specific equation to give an equal opportunity for the NDVI pixel values to be presented, and the 79-m resolution is equity-compared with the 30-m resolution datasets statistically, as shown in Eq (2):

$$\mathbf{DE} = \frac{\boldsymbol{\lambda DN}}{\sum \boldsymbol{DNs}} \times \mathbf{100} \quad (2)$$

Where *DE* is the dataset equality, λ *DN* is the digital number of the pixel value (NDVI value) of each pixel in a single satellite image, and the $\sum DNs$ is the sum of all pixel values (sum of all NDVI values) in the same satellite image. Then, this has been done across all the satellite images.

Negative values of NDVI (values nearer to −1) relate to non-vegetated surface, which normally represents water bodies, whereas, negative values near zero (0.0), for the most part, relate to barren territories of rock, sand or snow [45,61]. This will depend on the relative NIR and red reflectance of the particular rock and sand in a particular image, which rests on testing the cut-off values for the chosen images and areas [44,45]. Apparently, at the local coastal ecosystem, low positive values relate to bush and meadows of saltmarsh (roughly, 0.2 to 0.4), while high values demonstrate mixed and tropical mangroves and blended plants, for example, casuarina (values drawing closer to 1). The typical reach is between ca. −0.1 (for a not exceptionally green territory) to 0.6 (for an extremely green zone) [5,6,10,45].

Values under zero commonly do not have any ecological significance, thus, this paper considers the whole range −1.0 to 1.0, but it gives more attention to the range 0.0 to 1.0. Higher values provide a greater distinction between the red and near-infrared radiation recorded by the sensor, a condition connected with photosynthetically dynamic vegetation. Low NDVI values mean there is little distinction between the red and NIR signals. This happens when there is minimal photosynthetic activity, or when there is simply almost no NIR light reflectance (i.e., water reflections) [5,6,45].

2.2. Pixel value subtraction of NDVI change maps

The spatial distribution of NDVI change maps was calculated from the raster calculator expressions, which allows the power of basic algebraic expressions to be performed on raster maps [62,63]. An expression was written in which the earlier (1975) NDVI rasters, for example, were subtracted from the later (2015) NDVI sets to generate a raster representing spatial-NDVI changes over the study period, and so on for all the input images, to detect and demonstrate any trends. This is simply subtracting the pixels from each other within the same latitude and longitude to create new pixels at the same locations, but with the remaining values of NDVIs, whether positive or negative values, which will indicate spatial vegetation growth or decline, respectively.

To limit the errors that are often introduced by the choice of the start and finish time (for instance 1975 "as base-start point" and 2015 "as end change-compression point"), we have chosen nine starts and end points at five year intervals between 1975 and 2015 for more precise comparisons. Additionally, for more accuracy and validation, there is considerable literature in the remote sensing change detection and analysis field that looks at many ways to deal with multiple date datasets in an easier manner. Thus, we used a change vector (a visual method), which shows, for a pixel or

collection of pixels, the trajectory of change throughout the period. The use of change vector analysis is recognised as an optimised method for efficiently detecting and categorising the change distribution in pattern-boarder over time, and has been successfully applied to NDVI time-trajectories over an area [64–66].

2.3. Regression model

Statistical regression was used to explore the relationship between NDVIs as an indicator of wetland vegetation and a range of potential climate drivers for corresponding years. A multiple-linear regression model was employed by exporting the RS data into RStudio (for each study site) where they were combined, with consideration to their time scale order, in the dataset to maximize variability across the variables explored.

For each data case (the three case studies), there was an RS measure of NDVI vegetation (dependent variable) regressed against the values of three climatic indicators; temperature, precipitation, and sea level rise, as well as data on sedimentation rates (independent variables). The sedimentation data for the Towamba, Wandandian and Comerong sites were obtained from previous research that concentrated on the geomorphic dynamism of these sites [16,17,27,28,67,68]. Data pre-processing has been applied to the whole dataset. Since this paper is focused on the permanent vegetation state that resulted from the environmental conditions over years, we used the five-year-average technique of calculating the NDVIs, climatic, and sedimentation rates, and then run the regression model. For example, the NDVI values for 1980 are gained by averaging pixels over a spatial area for the five years before 1980 (1976–1980). This has been applied to all NDVI series (except 1975, which was based on the prior three years only). The same time-averaging has been done for all other variable datasets to gain the averages of climate and sedimentation conditions. Then the regression model plotted the average (mean) pixel values for each year of the NDVIs, climatic, and sediment rate factors at each location to determine the coefficients of variation β0 to β4, and the variation proportions accounted for by each regression model. The regression procedure was achieved by inputting data cases into Eq (3):

$$\mu_{(i)} = \beta_0 + \beta_1 T_{1(i)} + \beta_2 R_{2(i)} + \beta_3 SLR_{3(i)} + \beta_4 geo_{4(i)} + e_{(i)} \qquad i = 1, \ldots, n \qquad (3)$$

Where μ is the average of the NDVI pixel values for the year (dependent variable), T_1 (temperature), R_2 (rain), SLR_3 (sea level rising), and geo_4 (sedimentation rate as a geomorphic factor) are the independent variables, $e_{(i)}$ is the independent, normally distributed error term, n is the number of pixels each year at each study site, and $\beta_0, \ldots, \beta_4$ are coefficients estimated.

Separate regressions were run for each of the case study sites on the southern NSW coast.

3. Results

3.1. Ecosystem dynamics (vegetation/NDVI trends and statistical regression models)

Visualizing and analysing the vegetation dynamics of the three study sites has been accomplished using NDVI derived from Landsat data over the last 40 years (1975–2015; Figures 7–13). NDVI has rearranged the pixel values from the Landsat data from a multispectral scale of 0–255 to the NDVI form of −1 to 1. Visually, the NDVIs have resulted in Figures 7a, 10a and 12a that show a clear trend of

dynamic "brownness and greenness (−1 to 1)" land-cover changes at the study sites over time. This can determine the whole land ecological and geomorphological cover dynamics. Statistically, however, this paper has focused more on the ecological side, as presented by the vegetation dynamics (greenness), so only the positive values have been interpolated statistically (0 to 1) to represent greenness canopies (Figures 7b, 10b and 12b).

In general, the NDVI analyses have shown noticeable overall NDVI value increases at Towamba estuary and Wandandian delta (Figures 7 and 10) whereas, at Comerong Island, a decline in the overall NDVI values occurred over the study period (Figure 12).

3.1.1. Towamba estuarine ecosystem

The Towamba ecosystem has been analysed for its vegetation canopy dynamics using the NDVI and Landsat data from 1975 to 2015 (Figure 7).

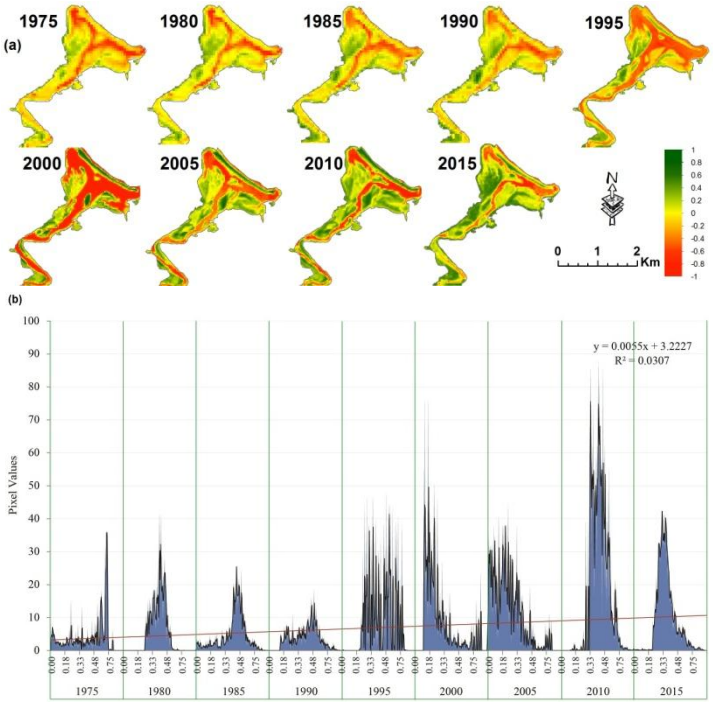

Figure 7. Ecosystem dynamics at a landscape level for the Towamba estuary investigations from 1975 to 2015 represented by the NDVI values. (a) Maps show a clear vegetation growth trend in all estuary classes (−1 to 1 of the NDVI values); (b) histograms of the statistical analysis of the greenness side only (0 to 1 values of the NDVI scale) show a significant trend of vegetation growth over the study period. *On the y axis, all NDVI positive values have been rescaled from 0–1 to 0–100 using Eq (2) to make whole numbers. On the x axis, the original range of the NDVI (pixel scales 0 to 1) is displayed, which is recorded for each year and separated by the green vertical line.

In general, Figure 7 shows significant estuarine ecosystem growth and changes within the last forty years in all eco-geomorphic land-covers, including the vegetation canopy in graded green, sandspit patterns in yellow, and water bodies in red (see Figure 7a). More accurately, a concentrated statistical

vegetation analysis (see Figure 7b) has shown a clear growth of the greenness of the land-covers.

Figure 7 shows the spatial distribution of the NDVI values at the Towamba estuary, which has gradually increased overall during the last four decades, with some fluctuations (e.g., 1990–2000). Relating these changes over time to the relevant climatic trends can be examined by regressing them with the NDVI trends. Linear regression model analysis has been done using RStudio software, and Figure 8 and Table 5 detail the relationship of averaged climatic and geomorphic factors (temperature, precipitation, sea level, and sedimentation rates) as independent variables that could affect the averaged NDVI trends (as the dependent variable) at the Towamba site.

From the scatterplot (Figure 8a) and Table 5 we can see a significant positive linear relationship between the dependent variable (NDVI) and the explanatory variable (time in years). An NDVI value of 5.21×10^{-06} has a weak positive linear relationship with temperature, which is not significant at the 95% level (Figure 8b). Rainfall is also not significant at the 95% level and it shows a very weak negative linear relationship with NDVI (Figure 8c). However, there is a moderate positive linear relationship between the sea level and NDVI (Figure 8d) that is statistically significant. Finally, plotting NDVI vs. sedimentation rates (Figure 8e) illustrates a significant strongly-positive linear relationship between the variables.

Table 5. Correlation summary of the regressed variables for the Towamba site, shows the R^2, *p*-value and the impact level.

Variables	R^2	*p*-value	Effects
Year	0.9499	5.206×10^{-06}	P
Temperature	0.2791	0.08261	P*
Rain	−0.1078	0.652	N*
Sea levels	0.686	0.003571	P
Sediment rates	0.8408	0.0003113	P

*Means not significant, P is positive and N is negative.

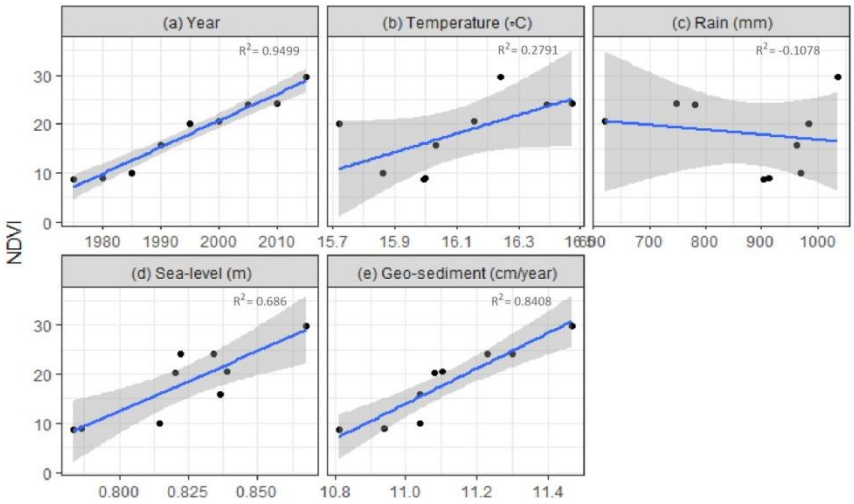

Figure 8. Results of the linear regression model show positive relationships between NDVI and (a) time; (b) temperature; (c) with rainfall records; (d) rising sea level; (e) the sedimentation rates, but a negative relationship. The grey area is the standard deviation of the data.

3.1.2. Wandandian estuarine delta

Analysis of the Wandandian ecosystem dynamics at the landscape level is represented by its vegetation canopy changes, which have been monitored using the NDVI calculated from the past four decades of Landsat data (Figure 9).

Figure 9 shows significant estuarine deltaic ecosystem growth during the study period (1975–2015) in all eco-geomorphic land-cover classes, including vegetation canopies shown in graded green, sandspit patterns in yellow, along with a decrease in water bodies in red (Figure 9a). Objectively, a concentrated statistical vegetation analysis has shown a significant growth of the greenness of the canopies (Figure 9b).

Figure 9 supports the literature findings of deltaic growth [33] in shorter-term variability, and shows a clear vegetation growth over time, both visually and statistically, for the whole eco-geomorphic platform. The NDVI spatial and statistical distribution trends show a significant overall increased brownness and greenness during the last four decades (Figure 9). This has documented the overall ecosystem growth, with a clear smoothing of the spatial distribution. A slight fluctuation occurred during 1990 to 2000 (Figure 9a).

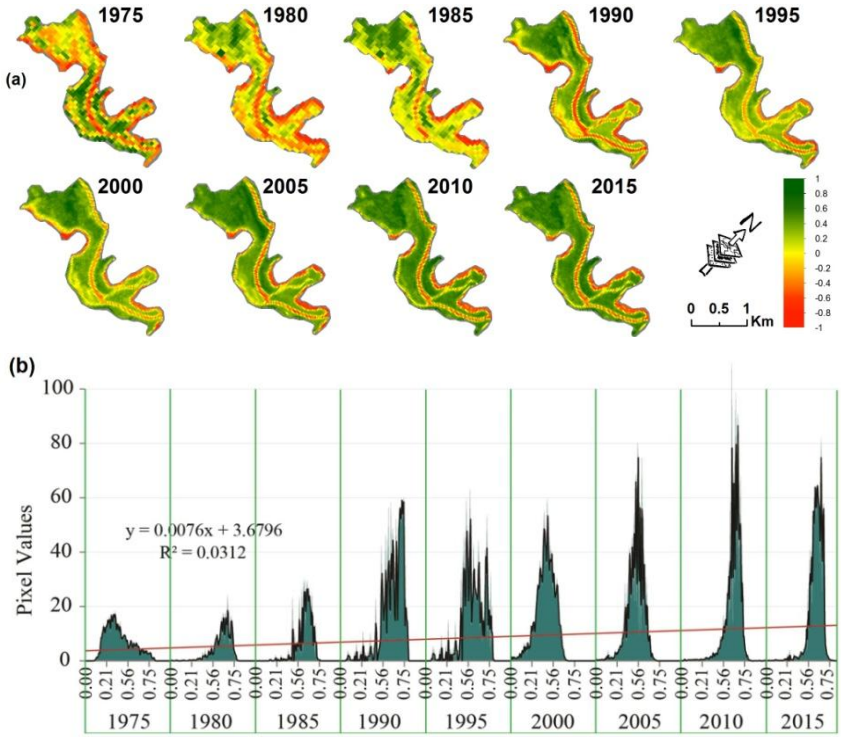

Figure 9. Ecosystem dynamics of the Wandandian site investigations from 1975 to 2015 as presented by the NDVI values. (a) Visual display shows a clear growth trend of all eco-geomorphic estuary classes (−1 to 1 of the NDVI values); (b) histogram of the statistical analysis of the greenness side only (0 to 1 of the NDVI values) showing a statistically significant increased trend of vegetation growth on the Wandandian delta over the study period. *On the y axis, all NDVI positive values have rescaled from 0–1 to 0–100 using Eq (2) to make whole numbers. On the x axis, the original range of the NDVI (pixel scales 0 to 1) is displayed, which is recorded at each year and separated by the green line.

Results from the linear regression analysis model provide details of the climate-related factors plus the sedimentary processes that could affect the NDVI trends at the Wandandian site (Figure 10 and Table 6).

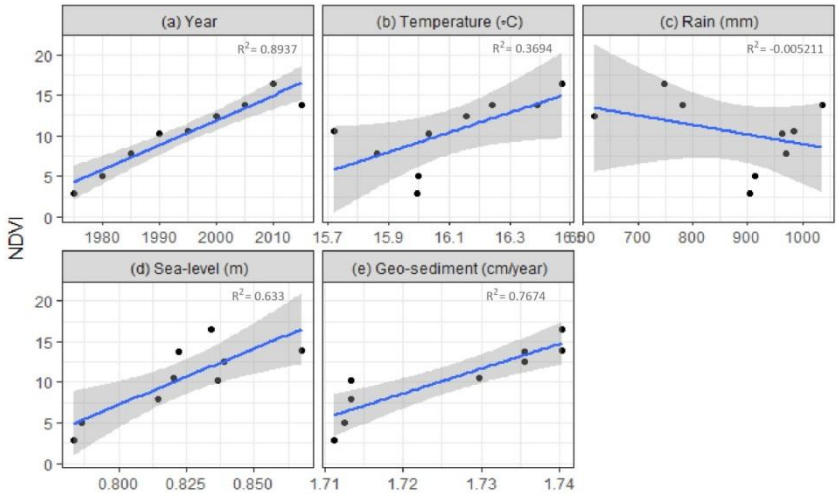

Figure 10. Results of the linear regression model with different significant *p*-values, showing a positive relationship between NDVI and (a) time; (b) temperature; (c) with rainfall records; (d) rising sea level; (e) sedimentation rates, but a negative relationship. The grey area is the standard deviation of the data.

A strong positive linear relationship is illustrated between the dependent variable (NDVI) and the explanatory variable (time in years; Figure 10a, Table 6). Secondly, the relationship between the NDVI and temperature (Figure 10b) is significant at the 95% level (*p*-value = 0.0486) indicating that temperature has a moderate positive linear relationship with NDVI. Rainfall does not have a significant effect on NDVI (Figure 10c). In contrast, there is a strong positive linear relationship between NDVI and SLR (Figure 10d) and between NDVI and the sedimentation rate.

Table 6. Correlation summary of the Wandandian site, showing the R^2, *p*-value and the effects value.

Variables	R^2	*p*-value	Effects
Year	0.8937	7.407×10^{-05}	P
Temperature	0.3694	0.04856	P
Rain	−0.005211	0.3414	N*
Sea levels	0.633	0.006316	P
Sediment rates	0.7674	0.001207	P

*Means not significant, P is positive and N is negative.

3.1.3. Comerong Island

Figure 11 shows the ecosystem dynamics, at a landscape scale, of Comerong Island as represented by the vegetation canopy based on the NDVI reclassification of the Landsat data from 1975 to 2015.

Eco-geomorphic land-cover classes on Comerong Island show a slight decline in all ecosystem land-covers over the last forty years (Figure 11a). Statistically, Figure 11b shows a clear decrease in the land-cover greenness by concentrating statistical analysis on the vegetation side only (0 to 1).

Figure 11 confirms the literature findings on Comerong Island of high southern shoreline erosion rates [37] and slight northern sandspit growth [69]. The greenness trend shows a slight decline on Comerong Island during the past 40 years, with a clear spatial heterogeneity of fluctuations over the island and its shorelines. The NDVI spatial distribution on the island (Figure 11) has gradually decreased during the last four decades, with some fluctuations with higher greenness being recorded (e.g., 1975 and 2010), and then declining in 2015.

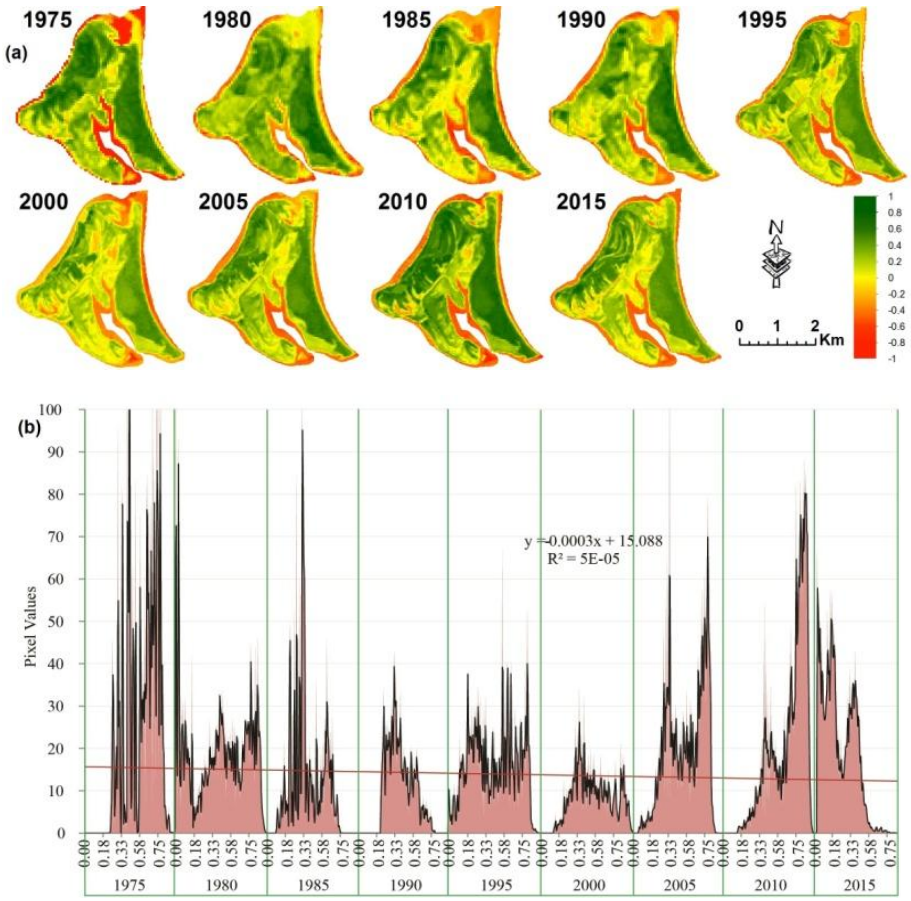

Figure 11. Ecosystem dynamics of the Comerong site investigation from 1975 to 2015 presented as NDVI values. (a) Shows a fluctuated visual declining trend of the island classes overtime (−1 to 1 of the NDVI values); (b) histogram of the statistical analysis of the greenness side only (0 to 1 of the NDVI values), that shows a slight statistical decline in the overall trend of vegetation dynamics over the study period. *On the y axis, all NDVI positive values have rescaled from 0–1 to 0–100 using Eq (2) to make whole numbers. On the x axis, the original range of the NDVI (pixel scales 0 to 1) is displayed, which has recorded at each year and separated by the green line.

Hence, a statistical regression model can be used to examine and estimate which climatic factors or sedimentary features have the most effect on the NDVI trends (Figure 12 and Table 7).

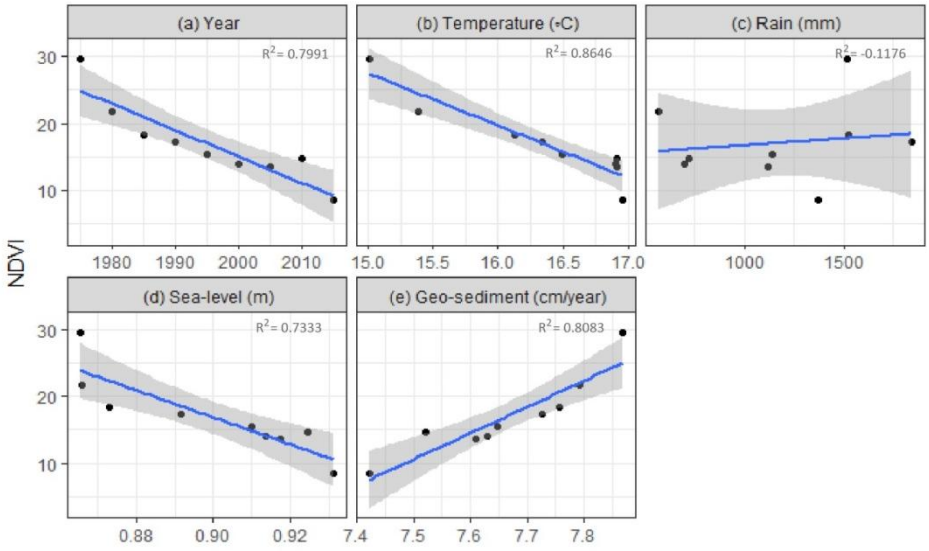

Figure 12. Results of the linear regression model show a negative relationship between NDVI and (a) time; (b) temperature; (c) rainfall records; (d) rising sea level, but a positive relationship with (e) sediment rates. The grey area is the standard deviation of the data.

The scatterplot (Figure 12a) of the NDVI over time demonstrates a strong negative linear relationship that is statistically significant at the 95% level (Table 7). There are also significant strong negative linear relationships between temperature and NDVI (Figure 12b) and between NDVI and sea level (Figure 12d). In contrast, a very weak positive linear relationship can be seen between NDVI and rainfall (Figure 12c). It can be concluded that NDVI may not be impacted by rainfall at Comerong Island. The scatterplot between sedimentation rate and NDVI (Figure 12e) suggests that there is a significant strong positive linear relationship between these variables.

Table 7. The Comerong site's summary of the linear model correlation, showing R^2, *p*-value and the effect relationship levels.

Variables	R^2	*p*-value	Effects
Year	0.7991	0.000714	N
Temperature	0.8646	0.0001749	N
Rain	−0.1176	0.7028	P*
Sea levels	0.7333	0.001977	N
Sediment rates	0.8083	0.0006031	P

*Means not significant, P is positive and N is negative.

3.2. Spatial distribution of NDVI change maps (using raster calculator)

Comparing NDVI maps from different time periods provides a measure of the vegetation canopy changes, as well as some geomorphic variables, over time by using the multi-map-algebra expression (in ArcPro using all nine imagery layers to avoid any one start and end point problems), and can be validated using the change vectors method (Figure 13). High values of the subtracted NDVI indices

equate to the presence of more vegetation; thus, simple comparisons have been drawn between values of the index on different dates to assess vegetation changes. For example, subtracting an index calculated for an earlier date from an index calculated for a later date yields positive values for vegetation gain (in green) and negative values for vegetation loss (in red). In this way, a map of the spatial distribution of vegetation change has been established for these coastal wetland cases in southeastern Australia.

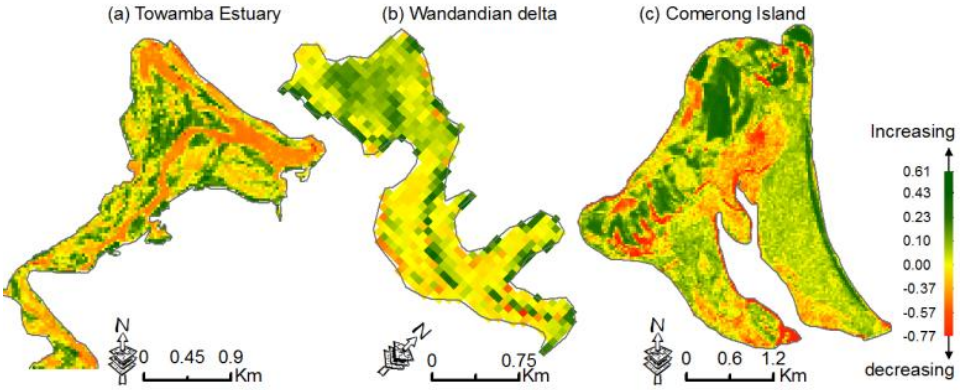

Figure 13. Raster calculator analyses (NDVI differences) showing the spatial distribution of NDVI changes at the study sites over time, using the map-algebra expression. The maps are based on the differences between the NDVI imagery pixel values of the nine start/end points between 2015 and 1975.

Figure 13 shows positive values in green are vegetation increases and negative values in red are vegetation decreases. Figures 13a and 13b illustrated clear increases in the NDVI values within the Towamba (ignoring the discharge channel in orange) and Wandandian sites, which reflect high vegetation growth rates at both sites. However, decreases in the emergent estuarine wetland vegetation canopy were detected on Comerong Island (Figure 13c) showing the decline as scaled from orange to red on the island landform itself.

4. Discussion

4.1. Towamba vegetation dynamics

4.1.1. Towamba NDVI trend

The Towamba ecosystem (at the landscape scale), and its habitat growth evidence, shows a clear spatial heterogeneity. The spatial distribution of the NDVI values in the Towamba estuary (Figure 7) has gradually increased overall during the last four decades, with some fluctuations (e.g., 1995–2000) that may relate to a flood event that occurred in late 1990 and eroded the active channel and low-lying sandspits. However, Figure 7 shows that erosion has affected the active channel bed more than the greenness cover over the estuary, and then the eco-geomorphic system started growing again. The overall growth represented by the mean NDVI (−1.0 to 1.0) over the study period increased by 9.5%, from 29.1% to 38.6% of the total wave reflections of the Towamba area (i.e., Figure 7b), whereas the

greenness portion (0.0 to 1.0) average increased, as well, by 5.9%, from 5.1% to 11%. This indicates that the Towamba estuary is growing both ecologically and geomorphologically. Interestingly, the bare geomorphic units (brownness; −1.0 to 0.0) have increased from 24% to 28.6%, at the Towamba site and are significantly larger than the greenness cover. Over four decades this might be due to the sedimentary characteristics of the estuary, whereby sediment infills the estuary providing ground on which vegetation can later become established.

4.1.2. Towamba regression model

The reason the linear regression test (Figure 8 and Table 5) shows a significant correlation between NDVI and all climate and sediment factors may be because the positive correlation with increasing sea level and sedimentation rate, as well as temperature, allows a longer growing season and higher photosynthetic productivity, in addition to gaining ground, geomorphologically, in this coastal system where water resources are available. Consequently, rainfall has not impacted the vegetation growth temporally since water-dependent plants mostly consist of mixed native plants on the elevated barrier island, which represents a very small area (~0.14 km^2, or 7% of the estuary). Sea level rise provides a significant positive effect in this correlation at the current rising rates, which may allow more accommodation for accumulating sediment and increasing ground-wetted areas, which would help develop ecosystem stability of habitable wetlands, as well as the other communities in the Towamba estuary. It might also reflect severe erosion during the 1974 floods on the east coast causing extensive scouring before this analysis started.

The Towamba site is really interesting since the increasing annual temperature trend shows an insignificant positive correlation (at the 95% level) with increases in the NDVI values, while it has a significant positive correlation at the other two study sites. These differences may relate to the higher latitude at Towamba, being located about 500 km south of Sydney. That has also resulted in different weather conditions, whereby the temperate oceanic climate (Cfb) has a slightly shorter growing season than other sites that have a warm oceanic to humid subtropical climate (Cfa). If temperature continues to increase at the Towamba site it should lead to a longer growing season since water and sediment resources are available to support a growth in the vegetation canopy.

4.2. Wandandian vegetation dynamics

4.2.1. Wandandian NDVI trend

Extension of the delta during the Holocene by continuous accumulation of sediments via Wandandian Creek from its partially-developed catchment has led to large areas in St Georges Basin being infilled, providing a good habitable estuarine area for a range of coastal ecosystems, such as wetland vegetation and associated communities. The NDVI spatial and statistical distribution trend shows a significant overall increase (brownness to greenness) during the last four decades (Figure 9). This has documented the overall ecosystem growth, with a clear smoothing of the spatial distribution. A slight fluctuation during 1990–2000 (Figure 9) may be related to the drought and low rainfall recorded from 1993 to 1995, as well as the flood events that hit the area from 1998 to 2000 (Figure 4) and may have caused some shoreline erosion, and the El Niño influences after 2010 [29].

The overall ecosystem growth represented by the mean total NDVI over the study period increased by 10.7%, from 8.4% to 19.1%, whereas, the greenness portion (0.0 to 1.0) has increased by 7.3%, from 6.9% to 14.2%. This indicates that the Wandandian site eco-geomorphic system is also growing ecologically and geomorphologically, but the ecological rate of growth is higher (7.3%) compared to the geomorphic growth of only 3.4% (from 1.5% to 4.9%). This could be because the low-lying wetlands have been well preserved and growing over the last few decades. However, it could also be related to the availability of sediment from the partially-developed catchment, and because the Wandandian delta is slowly accumulating under low wave energy conditions in the inner St Georges Basin [70] providing ideal habitat conditions for vegetation.

4.2.2. Wandandian regression model

Regression model analyses have shown clear vegetation growth over time for the whole ecosystem and statistically represent a preponderance of control by the three regressed climatic plus geomorphic factors on the NDVI values. The NDVI growth trend evidenced in the Wandandian delta can be interpreted from the linear regression test (Figure 10 and Table 6) which shows an insignificant negative relationship with rainfall, but a positive relationship with temperature, sea level rise and sedimentation rates. This indicates that increases in sea level have a significant positive correlation with the NDVI trend due to the long shorelines with low slope, as well as the large area of low-lying wetlands that include large mangrove and saltmarsh areas. The latter have a direct connection with St Georges Basin, whereby the rising sea level would influence the estuarine inundated areas in conjunction with the increasing sedimentation rates. Meanwhile, rainfall has a slight negative influence (−0.080 only) on vegetation radiation, especially on the elevated parts (~3–4 m) of the delta that are controlled by a shortage of water resources. Temperature has a significant positive affect on vegetation health as it provides a longer growing season.

4.3. Comerong Island vegetation dynamics

4.3.1. Comerong NDVI trend

Comerong Island has been generated by the Shoalhaven River as part of a wave-dominated delta, which also built the estuary and the associated ecosystems and habitats (e.g., unique wetlands) on the landward margin of the delta. Nowadays, however, although the Shoalhaven River has a very large catchment area of about 7200 km^2, which is the sixth largest catchment in NSW, the construction of the Tallowa dam restricted the amount of sediment delivered downstream to balance the erosion/deposition rates along the island's shorelines [16]. This has caused higher erosion rates along the western and southern sides of the island and resulted in a loss of area at some eco-geomorphic sites (e.g., shorelines and associated intertidal habitats like mangrove; [16,17,37]). This loss of vegetated area would effectively influence the vegetation radiation and, hence, the NDVI values. In contrast, a small part of the northern end of the island has been growing [69] at the same time because the original river mouth has been closed, allowing sedimentation to occur in this inactive region.

Comerong Island has been analysed for its ecosystem vegetation canopy dynamics using the NDVI and the Landsat datasets from 1975 to 2015. The greenness trend shows a slight decline on Comerong Island during the past 40 years, with a clear spatial heterogeneity of fluctuations over the

island and its shorelines. This could be related to specific climate events, such as El Niño, that hit eastern Australia between 2010 and 2012 and resulted in higher temperatures and flood events at this site [29]. Specifically, the middle and southern parts of Comerong Island have been more influenced than the other sides (Figure 11a).

The overall decrease represented by the mean total NDVI over the study period fell by 1.4%, from 24.6% to 23.2% (Figures 11a and 11b), whereas the greenness average decreased by 3.2%, from 18.3% to 15.2% (Figure 11b). This indicates that Comerong Island is deteriorating ecologically and geomorphologically. However, the rate of ecologic decline is higher, which may be due to: (i) geomorphic decline (caused by lower sediment supply and a rising sea level); (ii) leading to a decline in the vegetation growth trend; (iii) the rising temperature and falling precipitation that influences the more rain-dependent elevated habitats and mixed plant communities on the elevated 4–6 m high sandy barrier. Altogether, sedimentological and climatic factors have negatively affected Comerong Island with lost shoreline area, leading to vegetation/habitat losses as well.

4.3.2. Comerong regression

The linear model for Comerong Island (Figure 12 and Table 7) indicates that: (i) there is a significant negative relationship between the NDVI trend over time with temperature, rainfall, and sea level factors, which means a warmer climate with higher sea levels would result in a declining trend of vegetation greenness (NDVI values); (ii) higher temperature would increase drought conditions, particularly on the elevated barrier side. However, sedimentation rate has a significant positive effect on the NDVIs on Comerong Island's low-lying platforms.

4.4. Spatial distribution of NDVI change maps (using raster calculator)

Changes in vegetation distribution on these estuarine intertidal ecosystems have been explored over the study period (Figure 13) as follows: (i) the Towamba estuary ecosystem shows a slight increase in the NDVI green distribution, with some steady areas and losses on/around the main channel shorelines in yellow and orange, respectively; (ii) the Wandandian delta shows a clear NDVI increase in the northwestern parts with a mainly steady trend on the other parts of the delta [70]. These features are related to the availability of multiple water resources at these two study sites and the high sediment accumulation rates that result in geomorphic growth at both the Towamba estuary and Wandandian delta, which has provided a more suitable habitat for ecological developments [70]; (iii) Comerong Island, in contrast, has a clear NDVI increase on the north side of the island and a slight increase on the middle and barrier sides, that are both extending geomorphically [69]. Some areas show steady records in yellow. However, there has been a significant decline in NDVI values in the middle, west, and southern parts of the island, as shown in orange to red. These arose because of increased salinity introduced by the decline in Shoalhaven River discharge since the dam was constructed in 1976 [17], and shoreline erosion [16,17,37], as well as storm surge and regional drought conditions following cyclones in the 1990s and El Niño conditions since 2010 [29].

4.5. Regional comparisons

4.5.1. NDVI surface analyses and trends

The Towamba estuary is growing ecologically and geomorphologically, with the rate of geomorphic growth being faster and wider than the plant communities. Over the last four decades this reflects the sedimentary characteristics of the estuary, whereby sediment infills the estuary, providing ground on which vegetation can become established.

The Wandandian site eco-geomorphic system is also growing ecologically and geomorphologically, but the ecological rate of growth is higher (7.3%) than the geomorphic growth of only 3.4%.

In contrast, the NDVI spatial distribution on Comerong Island (Figure 11) has gradually decreased during the last four decades, with some fluctuations showing higher greenness (e.g., 1975 and 2010). This indicates that Comerong Island is deteriorating ecologically and geomorphologically, but the rate of ecological decline is higher. These changes can be attributed to sediment erosion and the rising sea level.

4.5.2. Regression model

The reactions of the dependent variable (NDVI) to the regressed independent factors (time, temperature, rainfall, sea level and sedimentation rates) are summarized in Table 8.

The variables time (year), rising sea level and sedimentation rate have significant effects on NDVI trends, whereas temperature and rainfall have insignificant effects on increasing the NDVIs on the Towamba site. At the Wandandian delta all the variables have significant positive effects on the NDVI index, except rainfall. In contrast, at Comerong Island, time, temperature, and sea level rise have significant negative impacts on the NDVIs, whereas rainfall has an insignificant effect, and sedimentation rate has a positive influence.

Table 8. The effect of five variables in three areas on NDVI at a 95% significance level.

Site	Time	Temperature	Rainfall	Rising Sea level	Sedimentation rates
Towamba	P	P*,†	N*	P	P
Wandandian	P	P	N*	P	P
Comerong	N	N	P*	N	P

*Means not significant, P is positive and N is negative († at Towamba site, temperature is significant at the 90% confidence level).

From all three study sites, at a 95% confidence level (which is the target of this research), estuarine ecosystems can be characterised as follows:

- Rainfall does not have a significant effect on NDVI index.
- The effect of sedimentation rates is positive and significant on the NDVIs.
- The temperature effect is significant within elevated estuarine platforms, such as the Wandandian and Comerong sites, whereas it is insignificant at low-laying surfaces, like the Towamba site situation.
- SLR is playing varies roles within estuarine platforms according to the sediment erosion/deposition rates. For instance, at Comerong Island, the SLR has a significant negative effect on NDVI, but it has a positive effect in the other regions.

Generally, the correlation between NDVI and the climatic and geomorphic factors is very significant at Towamba, Wandandian and Comerong, indicating that these factors (except the

remaining R^2 of other non-regressed factors) are the main controllers that will disturb the NDVI at such intertidal landforms during the 21st century worldwide.

4.5.3. NDVI change maps

The spatial distribution of NDVI change maps (Figure 13) were important to show, easily and clearly, the change in vegetation distribution at each study site, which may be informative about the causes and/or drivers of change at the local scale. NDVI change maps have effectively employed the map-algebra expression (raster calculator tool) to Landsat datasets, to show a clear pattern of changes at particular areas over time [62,71].

The zoned changes, which have been detected, have smoothly interpolated, and mapped the dynamic changes of NDVI distributions over the study sites/period. This has allowed these zoned changes to be related to the responsible factors, such as water shortage on some elevated parts of the Wandandian delta, and the erosion of shorelines around Comerong Island.

The resultant NDVI maps have shown clear vegetation changes over time, as well as other land cover attributes (water bodies, sandspit). Furthermore, more accurate results can be gained by understanding and statistically comparing these greenness (vegetation) changes with climate-related factors, especially when using the positive NDVI values (0.0–1.0) that represent the vegetation canopy, and ignoring the negative values (−1.0 to 0.0) that represent the bare-lands and water. The regression model has shown the significant impact that the environmental changes have on the NDVIs, and indicates that some non-regressed factors (accounting for the remaining R^2) are affecting the vegetation of these areas. Moreover, mapped NDVI distribution dynamics over the study sites/period has clearly indicated the change zones, which need more investigation to determine the responsible causes within these sections.

5. Conclusions

Although the climatic and sea level factors have slightly different values at each study site, all sites have tended to show an increase in temperature and sea level, and a decline in rainfall. This reflects the homogeneous coastal conditions that simulate the global trends with the small differences being related to the latitude at each site. However, a clear variation of vegetation reaction has occurred at these three coastal sites, resulting in different NDVI trends and different correlations with the climatic and sea level factors. Consequently, the NDVI may have been affected by another independent variable, which has been identified as the sedimentation rate since it impacts on the area of vegetation reflection. Hence, the geomorphological characteristics underlying the vegetation cover have a significant impact in such highly-dynamic intertidal estuarine landforms subject to active erosion and deposition processes.

Another finding of this research is that by using the maximum available RS datasets, which exhibit a variety of spatial resolutions through the study period, fixable and fairly comparable in pixels processing terms, though. A specific dataset equality equation has been designed for NDVI-imagery and allows the 79 m and 30 m resolution data to be compared statistically over time.

The NDVI was used to assess the sensitivity of coastal wetland vegetation at the study sites to the main climatic variables. Values of this index were calculated from Landsat 1–8 imagery across a range of wetland vegetation types growing on various geomorphic-sedimentary landforms.

The unique wetland habitats of coastal ecosystems are among the most productive and sensitive natural ecosystems on Earth. They are highly responsive to environmental pressures, both ecologically and geomorphologically. Climate change (particularly temperature, rainfall, and sea level rise) and coastal geomorphic processes (sedimentation) have clearly impacted most ecosystems worldwide. The vegetation canopy indicator has successfully represented the coastal ecosystem dynamics at the landscape scale. This exploratory study has investigated the response of coastal vegetation to climate changes and sediment rates along the three sensitive coastal ecosystems on the southeastern Australian coast. The published literature has argued that the Normalised Difference Vegetation Index (NDVI) is the best vegetation dynamic representative. Geoinformatic techniques including Landsat imagery modelling and subsequent statistical analyses have provided a qualitatively significant outcome that can be used to offer possible sustainable management solutions with worldwide applications.

Acknowledgments

This project has been financially funded by the GeoQuEST Research Centre, University of Wollongong, Australia. The reviewers and editor are thanked for their suggestions for improvements to the earlier version of this paper.

Conflict of interest

The authors declare no conflict of interest.

References

1. Costanza R, (1999) Ecological sustainability, indicators, and climate change, In: *IPCC Expert Meeting on Development, Equity and Sustainability*, Colombo, Sri Lanka, Citeseer.
2. Pittock AB (2003) Climate change: An Australian guide to the science and potential impacts. *Aust Greenhouse Off Canberra*.
3. Zinnert J, Shiflett S, Vick J, et al. (2011) Woody vegetative cover dynamics in response to recent climate change on an Atlantic coast barrier island: A remote sensing approach. *Geocarto Int* 26: 595–612.
4. IPCC, (2014) Climate Change 2014: Synthesis Report. In: Core Writing Team, R.K. Pachauri and L.A. Meyer, Eds., *Contribution of Working Groups I, II and III to the Fifth Assessment Report of the Intergovernmental Panel on Climate Change*, Geneva, Switzerland, 151.
5. Goward SN, Prince SD (1995) Transient effects of climate on vegetation dynamics: Satellite observations. *J Biogeography* 22: 549–564.
6. Donohue RJ, Mcvicar TR, Roderick ML (2010) Climate-related trends in Australian vegetation cover as inferred from satellite observations, 1981–2006. *Global Change Biology* 15: 1025–1039.
7. Woodroffe CD (1990) The impact of sea-level rise on mangrove shorelines. *Prog Phys Geogr* 14: 483–520.
8. Michener WK, Blood ER, Bildstein KL, et al. (1997) Climate change, hurricanes and tropical storms, and rising sea level in coastal wetlands. *Ecol Appl* 7: 770–801.
9. Scavia D, Field JC, Boesch DF, et al. (2002) Climate change impacts on US coastal and marine ecosystems. *Estuaries* 25: 149–164.

10. Day JW, Christian RR, Boesch DM, et al. (2008) Consequences of climate change on the ecogeomorphology of coastal wetlands. *Estuaries Coasts* 31: 477–491.
11. Meyssignac B, Cazenave A (2012) Sea level: A review of present-day and recent-past changes and variability. *J Geodyn* 58: 96–109.
12. Mitsch WJ, Gosselink JG (2015) Wetlands 5th edition, Wiley, New Jersey, 744pp.
13. NCCMA (1998) The role of wetlands Fact Sheet Project 1559. *North Central Catchment Management Authority*, Huntly, Victoria, 2pp.
14. DSE, (2007) Index of Wetland Condition (Review of wetland assessment methods), Department of Sustainability and Environment: S.A. Melbournethe, Victorian Government.
15. Al-Nasrawi AKM, Jones BG, Alyazichi YM, et al. (2015) Modelling the future eco-geomorphological change scenarios of coastal ecosystems in southeastern Australia for sustainability assessment using GIS, In: *ACSUS 2015 Proceedings: The Second Asian Conference on the Social Sciences and Sustainability,* Japan, 0196.
16. Al-Nasrawi AKM, Jones BG, Alyazichi YM, et al. (2016) Civil-GIS incorporated approach for water resource management in a developed catchment for urban-geomorphic sustainability: Tallowa Dam, southeastern Australia. *Int Soil Water Conserv Res* 4: 304–313.
17. Al-Nasrawi AKW, Jones BG, Hamylton SM (2016) GIS-based modelling of vulnerability of coastal wetland ecosystems to environmental changes: Comerong Island, southeastern Australia. *J Coastal Res* 2016: 33–37.
18. Hughes L (2003) Climate change and Australia: Trends, projections and impacts. *Aust Ecol* 28: 423–443.
19. Nicholls RJ (2004) Coastal flooding and wetland loss in the 21st century: Changes under the SRES climate and socio-economic scenarios. *Global Environ Change* 14: 69–86.
20. Blay J (1944) On Track: Searching out the Bundian Way, Eden local history reference collection. Sydney: NewSouth Publishing.
21. Wright LD (1970) The influence of sediment availability on patterns of beach ridge development in the vicinity of the Shoalhaven river delta, N.S.W. *Aust Geogr* 11: 336–348.
22. Hopley CA (2013) Autocyclic, allocyclic and anthropogenic impacts on Holocene delta evolution and future management implications: Macquarie Rivulet and Mullet/Hooka Creek, Lake Illawarra, New South Wales. PhD thesis, University of Wollongong, Australia, 338.
23. OEH (2013) Assessing estuary ecosystem health: Sampling, data analysis and reporting protocols: NSW Natural Resources Monitoring, Evaluation and Reporting Program. State of NSW and Office of Environment and Heritage, 3–38.
24. Kirkpatrick S, (2012) The Economic Value of Natural and Built Coastal Assets: Part 2: Built Coastal Assets, In: *Australian Climate Change Adaptation Research Network for Settlements and Infrastructure,* National Climate Change Adaptation Research Facility.
25. Pendleton LH (2010) The economic and market value of coasts and estuaries: What's at stake? *Economic* 175.
26. Roy PS, Williams RJ, Jones AR, et al. (2001) Structure and function of south-east Australian estuaries. *Estuarine Coastal Shelf Sci* 53: 351–384.
27. Al-Nasrawi AKM, Hamylton SM, Jones BG (2018) Spatio-temporal assessment of anthropogenic and climate stressors on estuaries using a GIS-modelling approach for sustainability; Towamba estuary, southeastern Australia. *Environ Monit Assess J.*

28. Al-Nasrawi A, Hopley C, Hamylton S, et al. (2017) A Spatio-Temporal Assessment of Landcover and Coastal Changes at Wandandian Delta System, Southeastern Australia. *J Mar Sci Eng* 5: 55.
29. Bureau of Meterology. NSW Weather, 2017. Available from: http://www.bom.gov.au.
30. Dean LF, Deckker PD (2013) Recent benthic foraminifera from Twofold Bay, Eden NSW: Community structure, biotopes and distribution controls. *J Geol Soc Aust* 60: 475–496.
31. DPI/OW. NSW Office of Water—NEW Government—Department of Primary Industries, 2017. Available from: http://www.water.nsw.gov.au/.
32. Hudson JP, (1991) Late Quaternary Evolution of Twofold Bay, Southern New South Wales, In: *Department of Geography*, University of Sydney: Unpublished.
33. Jones CAHBG (2006) Holocene stratigraphic and morphological evolution of the Wandandian Creek delta, St Georges Basin, New South Wales. *J Geol Soc Aust* 53: 991–1000.
34. Kingsford RT (1990) The effects of human activities on shorebirds, seabirds and waterbirds of Comerong Island, at the mouth of the Shoalhaven River. *Wetlands* 9: 7–12.
35. Christian AT, Hill SM (2002) Regolith-landform mapping of the Shoalhaven River Delta and hinterland, NSW: Towards a model for landscape change and management. *Regolith Landscapes East Aust* 8–13.
36. Umitsu M, Buman M, Kawase K, et al. (2001) Holocene palaeoecology and formation of the Shoalhaven River deltaic-estuarine plains, southeast Australia. *Holocene* 11: 407–418.
37. Thompson CM, (2012) Recent Dynamic Channel Adjustments of Berrys Canal Shoalhaven Region, New South Wales Approach, In: *B.Env.Sc. thesis*, University of Wollongong.
38. DEE. Coasts and oceans: Ecosystem conditions, 2006. Available from: https://www.environment.gov.au/node/21960.
39. Bureau of Meteorology. Climate classification of Australia, 2017. Available from: http://www.bom.gov.au/climate/.
40. Fensham RJ, Fairfax RJ, Archer SR (2005) Rainfall, land use and woody vegetation cover change in semi-arid Australian savanna. *J Ecol* 93: 596–606.
41. Semeniuk C, Semeniuk V (2013) The response of basin wetlands to climate changes: A review of case studies from the Swan Coastal Plain, south-western Australia. *Hydrobiologia* 708: 45–67.
42. KNMI-Climate_Explorer. Select a monthly time series, 2018. Available from: https://climexp.knmi.nl/selectstation.cgi?id=someone@somewhere.
43. Raynolds M, Magnússon B, Metúsalemsson S, et al. (2015) Warming, sheep and volcanoes: Land cover changes in Iceland evident in satellite NDVI trends. *Remote Sens* 7: 9492–9506.
44. Weier J, Herring D (2000) Measuring Vegetation (NDVI & EVI). Available from: http://earthobservatory.nasa.gov/Features/MeasuringVegetation/.
45. Pettorelli N, Vik JO, Mysterud A, et al. (2005) Using the satellite-derived NDVI to assess ecological responses to environmental change. *Trends Ecol Evol* 20: 503–510.
46. Church JA (2013) Projections of sea level rise IPCC AR5. *Clim Change* 2013: 1137–1216.
47. Gedan KB, Kirwan ML, Wolanski E, et al. (2011) The present and future role of coastal wetland vegetation in protecting shorelines: Answering recent challenges to the paradigm. *Clim Change* 106: 7–29.
48. Costanza R, Pérez-Maqueo O, Martinez ML, et al. (2008) The value of coastal wetlands for hurricane protection. *Ambio* 37: 241–248.
49. Lee SY, Rjk D, Young RA, et al. (2006) Impact of urbanization on coastal wetland structure and function. *Aust Ecol* 31: 149–163.

50. Department of Environment, (2010) Riverine Ecosystems, Southern river Region, In: *State of the Catchments*, New South Wales Government.
51. Thom BG (1967) Mangrove ecology and deltaic geomorphology: Tabasco, Mexico. *J Ecol* 55: 301–343.
52. Deconto RM, Pollard D (2016) Contribution of Antarctica to past and future sea-level rise. *Nature* 531: 591–597.
53. Neumann B, Vafeidis AT, Zimmermann J, et al. (2015) Future Coastal Population Growth and Exposure to Sea-Level Rise and Coastal Flooding-A Global Assessment. *PloS One* 10: e0118571.
54. Pachauri RK, Team CW, Meyer LA (2014) Climate Change 2014: Synthesis Report. Contribution of Working Groups I, II and III to the Fifth Assessment Report of the Intergovernmental Panel on Climate Change. *J Romance Stud* 4: 85–88.
55. Bureau of Meterology-NSW. Tide Gauge Metadata and Observed Monthly Sea Levels and Statistics, 2017. Available from: http://www.bom.gov.au/oceanography/projects/ntc/monthly/.
56. USGS. EarthExplorer, 2017. Available from: http://earthexplorer.usgs.gov/.
57. USGS-Landsat. Landsat Collections, 2017. Available from: http://landsat.usgs.gov//landsatcollections.php.
58. Nguyrobertson AL, Gitelson AA (2015) Algorithms for estimating green leaf area index in C3 and C4 crops for MODIS, Landsat TM/ETM+, MERIS, Sentinel MSI/OLCI, and Venμs sensors. *Remote Sens Lett* 6: 360–369.
59. Peng Y, Nguy-Robertson A, Arkebauer T, et al. (2017) Assessment of canopy chlorophyll content retrieval in maize and soybean: Implications of hysteresis on the development of generic algorithms. *Remote Sens* 9: 226.
60. Feng T, Fensholt R, Verbesselt J, et al (2015) Evaluating temporal consistency of long-term global NDVI datasets for trend analysis. *Remote Sens Environ* 163: 326–340.
61. Curtis E (2016) The use of Landsat derived vegetation metrics in Generalised Linear Mixed Modelling of River Red Gum (Eucalyptus camaldulensis) canopy condition dynamics in Murray Valley National Park, NSW, between 2008 and 2016. University of Wollongong, Wollongong, Australia, 148.
62. Cordeiro JPC, Câmara G, Moura UF, et al. (2005) Algebraic Formalism over Maps. *Geoinfo* 2008: 49–65.
63. Esri. A quick tour of using Map Algebra—ArcGIS Help | ArcGIS Desktop, 2017. Available from: http://desktop.arcgis.com/en/arcmap/latest/extensions/spatial-analyst/map-algebra/a-quick-tour-of-using-map-algebra.htm.
64. Lambin EF, Strahlers AH (1994) Change-vector analysis in multitemporal space: A tool to detect and categorize land-cover change processes using high temporal-resolution satellite data. *Remote Sens Environ* 48: 231–244.
65. Zanchetta A, Bitelli G (2017) A combined change detection procedure to study desertification using opensource tools. *Open Geospatial Data Software Stand* 2: 10.
66. Li J, Xu B, Yang X, et al. (2017) Historical grassland desertification changes in the Horqin Sandy Land, Northern China (1985–2013). *Sci Rep* 7: 3009.
67. Al-Nasrawi A, Jones B, Hamylton S, (2015) Modelling changes of coastal wetlands responding to disturbance regimes (Eastern Australia), In: *Australian Mangrove and Saltmarsh Network Conference : Working with Mangrove and Saltmarsh for Sustainable Outcomes*, Wollongong, Australia: Australian Mangrove and Saltmarsh Network, 33.

68. Al-Nasrawi AKM (2017) Surface Elevation Dynamics Assessment Using Digital Elevation Models, Light Detection and Ranging, GPS and Geospatial Information Science Analysis: Ecosystem Modelling Approach. *Int J Environ* 131: 918–923.
69. Carvalho RC, Woodroffe C, (2013) Shoalhaven river mouth: A retrospective analysis of breaching using aerial photography, landsatimagery and LiDAR, In: *In Proceedings of the 34th Asian Conference on Remote Sensing 2013*, Indonesian Remote Sensing Society, Indonesia, 1–7.
70. Hopley CA (2004) The Holocene and beyond: Evolution of Wandandian Creek delta, St Georges Basin, New South Wales. BSc(Hons) thesis, University of Wollongong, Australia.
71. WRC, Wetland Mapping: Exercises—Create the NDVI Layer ArcMap 10. Water Resources Center (WRC), University of Minnesota [Online], 2012. Available from: https://www.wrc.umn.edu/sites/wrc.umn.edu/files/create_the_ndvi.pdf.

AIMS Press